

# Investigation of Vaporized Kerosene Injection and Combustion in a Supersonic Model Combustor

Xuejun Fan,\* Gong Yu,† Jianguo Li,‡ and Xinyu Zhang§  
*Chinese Academy of Sciences, 100080 Beijing, People's Republic of China*  
and  
Chih-Jen Sung¶  
*Case Western Reserve University, Cleveland, Ohio 44106*

**Injection and combustion of vaporized kerosene was experimentally investigated in a Mach 2.5 model combustor at various fuel temperatures and injection pressures. A unique kerosene heating and delivery system, which can prepare heated kerosene up to 820 K at a pressure of 5.5 MPa with negligible fuel coking, was developed. A three-species surrogate was employed to simulate the thermophysical properties of kerosene. The calculated thermophysical properties of surrogate provided insight into the fuel flow control in experiments. Kerosene jet structures at various preheat temperatures injecting into both quiescent environment and a Mach 2.5 crossflow were characterized. It was shown that the use of vaporized kerosene injection holds the potential of enhancing fuel-air mixing and promoting overall burning. Supersonic combustion tests further confirmed the preceding conjecture by comparing the combustor performances of supercritical kerosene with those of liquid kerosene and effervescent atomization with hydrogen barbotage. Under the similar flow conditions and overall kerosene equivalence ratios, experimental results illustrated that the combustion efficiency of supercritical kerosene increased approximately 10–15% over that of liquid kerosene, which was comparable to that of effervescent atomization.**

## Introduction

**I**N practical liquid-hydrocarbon-fueled scramjet operations, the most commonly adopted method to cool the engine would be regenerative cooling. The liquid fuel before being injected into the combustor is circulated through the walls of the combustor typically under high pressures of 35–70 atm (Ref. 1). It is also expected that the fuel temperature and its thermodynamic state vary with the flight Mach number and the different stages of the flight mission.<sup>2,3</sup> In the early flight stage, the amount of heat absorbed by the fuel is minimal; the liquid-hydrocarbon fuel would remain in the liquid state before entering the combustor. As the flight speed increases, the fuel temperature rises, and the fuel can transform to the vapor phase when exceeding its bubble point. If both fuel temperature and pressure are higher than the thermodynamic critical point, the fuel becomes supercritical. Further increasing the fuel temperature beyond 750 K would lead to thermal decomposition of the hydrocarbons in the fuel.<sup>1</sup>

When applying liquid fuel injection, the successful operation of a scramjet engine requires the processes of fuel vaporization, fuel-air mixing, self-ignition, and complete combustion to be accomplished within a limited residence time available in the combustor. As a consequence, extensive studies have explored various flame-holding schemes for providing a high-temperature radical source in the

recirculation zone with minimal stagnation pressure losses,<sup>4–11</sup> different atomization methods for achieving fast evaporation and fuel-air mixing,<sup>12–15</sup> and diverse chemical enhancements for shortening the characteristic reaction time through the use of partially cracked hydrocarbon fuels,<sup>16–18</sup> pilot hydrogen,<sup>4,5,14,19–22</sup> or plasma.<sup>23–25</sup> Along these lines, we have systematically examined the effects of injection strategy, pilot hydrogen, and cavity geometry on the performance of various liquid-kerosene-fueled model combustors.<sup>26,27</sup> It was also shown that a higher level of atomization can be achieved by using effervescent atomization, which can further promote the overall burning of kerosene in a supersonic airflow.<sup>27,28</sup>

As discussed earlier, with the use of regenerative cooling the liquid fuel could be vaporized before reaching the fuel injector. Even before the temperature is sufficiently high for the fuel to thermally react, the changes in thermophysical properties of the fuel, from saturated liquid to supercritical fluid, are expected to significantly affect the fuel injection process and the subsequent fuel-air mixing and combustion inside the supersonic combustor. Specifically, in the supercritical region the fuel exhibits liquid-like density, gas-like diffusivity, and pressure-dependent solubility.<sup>29</sup> As such, during injection the supercritical fuel can be directly transformed to the gaseous state corresponding to the local combustor condition. Either being supercritical or subcritical, one apparent benefit utilizing vaporized fuel injection is to bypass the atomization and vaporization processes. As a result, the overall fuel-air mixing could be enhanced. This would also in turn expand the combustion stability range by promoting self-ignition and extending the extinction limits.

Recognizing that experimental investigation involving the use of vaporized hydrocarbon injection in a supersonic model combustor with flame-holder cavities is meager, the present study aims to extend our previous endeavors on liquid-kerosene combustion in supersonic crossflows to assess the combustor performance with vaporized kerosene injection through systematic experimental characterizations. The effects of the changes in the fuel states on fuel injection process, self-ignition limit, and combustion efficiency of a kerosene-fueled supersonic model combustor were examined. A unique fuel delivery and injection system that covered a wide range of fuel injection modes, varying from liquid atomization to vaporized fuel injection, was also developed to carry out the experiments.

To accurately determine the flow rate of supercritical-pressure, high-temperature kerosene vapor and to control the fuel conditions

Presented as Paper 2004-3485 at the AIAA/ASME/SAE/ASEE 40th Joint Propulsion Conference and Exhibit, Ft. Lauderdale, FL, 11–14 July 2004; received 18 January 2005; revision received 31 May 2005; accepted for publication 6 June 2005. Copyright © 2005 by the American Institute of Aeronautics and Astronautics, Inc. All rights reserved. Copies of this paper may be made for personal or internal use, on condition that the copier pay the \$10.00 per-copy fee to the Copyright Clearance Center, Inc., 222 Rosewood Drive, Danvers, MA 01923; include the code 0748-4658/06 \$10.00 in correspondence with the CCC.

\*Associate Professor, Institute of Mechanics, 15 Zhongguancun Road, Haidian District; xfan@imech.ac.cn.

†Professor, Institute of Mechanics; yugong@imech.ac.cn. Member AIAA.

‡Professor, Institute of Mechanics; jgli@imech.ac.cn. Member AIAA.

§Professor, Institute of Mechanics; changxy@imech.ac.cn. Member AIAA.

¶Associate Professor, Department of Mechanical and Aerospace Engineering; cjs15@po.cwru.edu. Senior Member AIAA.

inside the fuel delivery and heating system, the thermophysical properties of kerosene as functions of pressure and temperature are needed. Because kerosene fuels are complex mixtures of alkanes, naphthenes, and aromatics, and their compositions vary constantly with time and place of production, it is impossible to define a precise composition of the kerosene fuel. Therefore, it is necessary to select a fuel surrogate to simulate various physical and chemical processes of kerosene for reproducibility in numerical and experimental studies.<sup>30–34</sup> An regressive study was conducted to identify a representative surrogate for the kerosene employed in the experimental investigation. The thermophysical properties of this kerosene surrogate were then theoretically calculated.

In the following text, we shall first describe our test facility, including the supersonic model combustor and the two-stage heating and delivery system for liquid/vaporized-kerosene injection. Determination of a three-species kerosene surrogate and theoretical calculations of the associated thermophysical properties will then be presented. Moreover, the procedure of calibrating the mass flow rate of supercritical-pressure kerosene vapor will be outlined. Additionally, the measured mass flow rate of kerosene vapor will be compared with the computed value. Subsequently, the injection of heated kerosene jet into quiescent atmosphere and a Mach 2.5 crossflow will be characterized using direct photograph and schlieren images, respectively. Finally, combustor performances using liquid-kerosene injection, effervescent atomization with hydrogen barbotage, and vaporized-kerosene injection will be compared and discussed.

## Facility Descriptions

### Test Facility

The experiments were conducted in a Mach 2.5 test facility that consisted of a vitiated air supply system, a multipurpose supersonic model combustor, and a kerosene delivery and heating system. The vitiated air was provided by burning hydrogen, oxygen, and air in the heater with the resulting oxygen volume fraction equal to that of the normal air. The facility operation, control, and data acquisitions were accomplished with a computer. It was capable of supplying heated air at stagnation temperatures of 800–2100 K and stagnation pressures of 0.7–1.3 MPa. Details of this facility were described in the study of Li et al.<sup>35</sup> The model combustor with a total length of 1070 mm, as shown in Fig. 1, was composed of three sections, including one nearly constant-area section with a cross section of 51 mm in height and 70 mm in width and two divergent sections. Two interchangeable integrated fuel injector/flameholder cavity modules were installed on both sides of the combustor, each with a depth of 12 mm, a 45-deg aft ramp angle, and an overall length-to-depth ratio of 7. In each module, there were five orifices of 0.9 mm (0.5 mm) diam designed for vaporized (liquid) kerosene injection, while there were five orifices of 1.0 mm diam available for pilot hydrogen injection. Both kerosene and pilot hydrogen were injected normally to the airflow upstream of the cavities. For light access and observation, a pair of quartz windows, each was 46 mm in height and 124 mm in length, were installed on both sides of the combustor near the location of cavity module.

The entire test facility was mounted upright on a platform and can be translated laterally and vertically. It usually took approximately 2.5 s to establish a steady Mach 2.5 airflow, and a typical run lasted around 7 s.

### Kerosene Delivery and Heating System

A major concern in the kerosene heating system is how to prevent the carbon formation, particularly because of pyrolytic cracking. The rate of this fuel coking is generally proportional exponentially to temperature and linearly to the residence time.<sup>1</sup> To minimize the fuel coking at high temperature, a two-stage heating system was designed, which is shown in Fig. 2. The first stage was a storage-type heater that can heat kerosene of 0.8 kg up to 570 K within a relative longer heating time (typically 20 min) with minor/negligible coking deposits, whereas the second stage was a continuous one, which was capable of rapidly heating kerosene to 830 K or higher. The residence time of vaporized kerosene within the second heater was very short, typically less than 2 s, thereby minimizing the extent of fuel coking.

The first-stage heater consisted of a 20-m-long stainless-steel tube of 20 mm inner diameter and 1.5-mm wall thickness, which was wound into a cylinder shape of 30 cm diam. The stainless-steel tube was wrapped with five 960-W heating tapes, which were controlled independently in order to achieve a uniform temperature distribution along the tube. On the other hand, the second-stage heater was heated electrically by directly passing a current through the stainless-steel tube at 80–100 dc voltages from a pulsed ac/dc welder power supply of 250 kW. In addition, the second-stage heater and the fuel injector were connected by 10-mm-diam tubes, which were also wrapped by heating tapes to reduce heat loss and avoid kerosene condensation before reaching the injector.

Two pneumatic valves (Swagelok, model No. SS6UM) were employed to turn on/off the two heaters promptly, as shown in Fig. 2. After each run, nitrogen was used to purge the residual kerosene inside the second-stage heater to eliminate carbon deposit accumulation. Two groups of K-type thermocouples, TC11–14 and TC21–24 in Fig. 2, were installed on the surface of or inserted into the heater tubes and were used to monitor and achieve the feedback control of fuel temperature distribution along the heating system.

Much effort was also devoted to establishing a quick delivery of the heated kerosene with stable fuel temperature and pressure. Figure 3 shows the performance of the two-stage heating system by plotting the time variations of temperature and pressure of the kerosene vapor at the exit of the second heater. In this case, the pneumatic valve between the first and second heaters was turned on at a reference time  $t$  of 2 s, and the fuel injection started at  $t = 4$  s. It is seen from Fig. 3 that the fuel temperature and pressure profiles leveled off in about 2 s after kerosene injection and were kept almost constant during the experiment duration.

To carry out accurate measurements of kerosene vapor flow rates, a sonic nozzle flowmeter of 2.15 mm in throat diameter was designed and installed between the second-stage heater and the fuel injector for real-time monitoring. The design of the flow-rate meter,

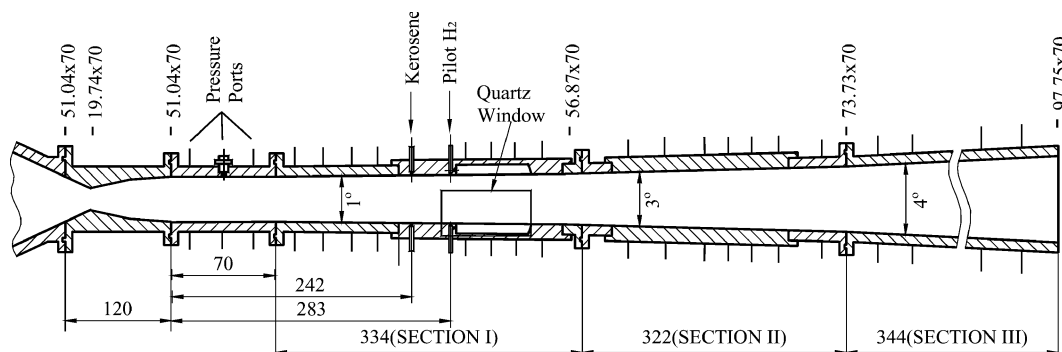


Fig. 1 Schematic of supersonic model combustor with kerosene/pilot hydrogen injection. All length dimensions are in millimeters.

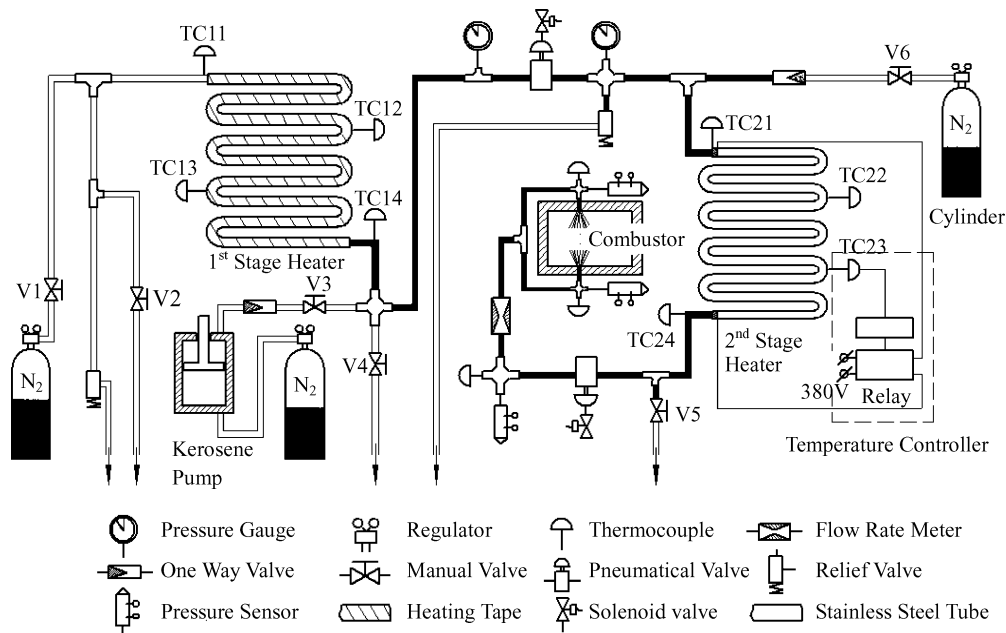


Fig. 2 Schematic of kerosene delivery and heating system.

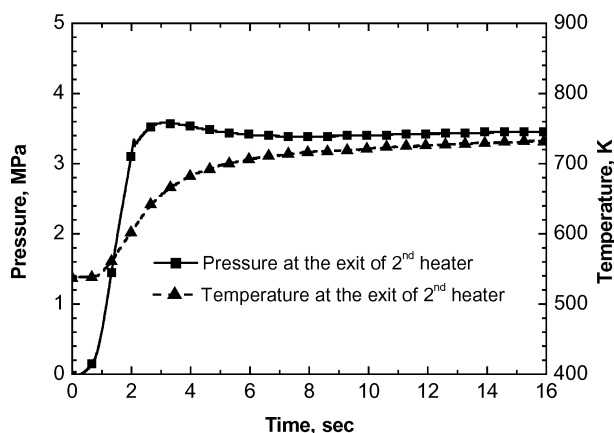


Fig. 3 Typical time variations of kerosene pressure and temperature measured at the exit of the second heater.

calibration procedure, and thermophysical property calculations of the kerosene surrogate are detailed in the following sections.

## Thermophysical Properties of Kerosene Surrogate

### Composition of Kerosene Surrogate

Depending on either the physical or chemical properties of the parent fuel that are to be simulated, the fuel surrogate can be categorized as a physical or a chemical surrogate. In the literature, a number of surrogates have been proposed for the common jet fuels.<sup>30–34</sup> For the present study, the determination of the mass flow rate of supercritical kerosene was of particular interest. Therefore, a physical surrogate was developed to match the thermophysical properties of the aviation kerosene employed in experiments, such as density, normal boiling point, and critical parameters.

Table 1 lists the measured mass fractions of various components of China no. 3 aviation kerosene employed herein. On a molar basis, it was approximately composed of 92.5% saturated hydrocarbons, 0.5% unsaturated hydrocarbons, and 7% aromatic hydrocarbons. As shown in Table 1, the major compounds are n-alkanes, monocycloalkanes, and aromatics. To match the compound class, it is desirable for the surrogate fuel to contain at least one representative compound from each class.<sup>30</sup> Among many candidates in n-alkanes and monocycloalkanes, n-decane and 1,3,5-trimethylcyclohexane

Table 1 Composition (mass basis) of China no. 3 aviation kerosene

Hydrocarbons	Values
Saturated	
Alkanes	52.2
Naphthenes	
Monocyclic	33.8
Bicyclic	6.0
Tricyclic	0.1
Total	92.1
Aromatic	
Alkyl benzenes	5.1
Indan and tetralin	1.3
Naphthalene	0.6
Naphthalene derivatives	0.9
Total	7.9
Total	100

were selected because their normal boiling temperatures are approximately 447 and 413 K, respectively, which are comparable to the measured dew temperature (~452 K) and bubble temperature (~415 K) of China no. 3 aviation kerosene. In addition, guided by Dagaut's three-component surrogate,<sup>31</sup> n-propyl-benzene was selected to represent the class of aromatic hydrocarbons. The molar fraction of each compound was initially chosen according to Table 1 and subsequently adjusted in order for the calculated values of density and critical parameters to match the experimental data. After several iterations, the final surrogate fuel consisted by mole of 49% n-decane, 44% 1,3,5-trimethylcyclohexane, and 7% n-propyl-benzene.

### Thermophysical Modeling of Kerosene Surrogate

In the vaporized kerosene injection with fuel state near or above the critical point, the fuel behaviors are very complex and sensitive to pressure and temperature variations. No single equation of states is available to fully represent the properties of the fuel over the entire range of temperatures and pressures. Thus, the thermophysical properties of the present three-species surrogate were computed using the NIST SUPERTRAPP<sup>36</sup> software package based on the extended corresponding states principle.<sup>29,37</sup> The corresponding states principle assumes that the equations of states when presented in terms of the reduced variables (normalized by the corresponding critical value) for various fluids follow exactly the same pattern and can be

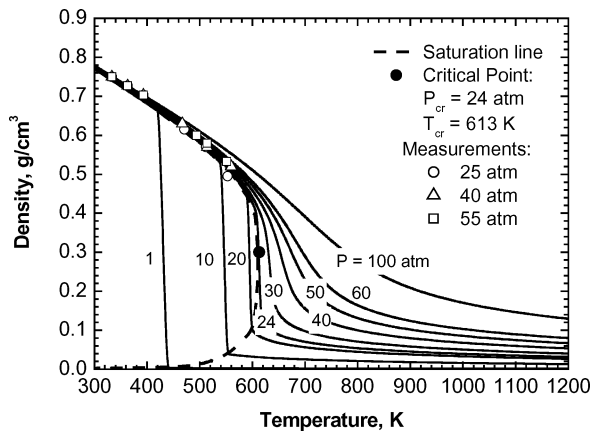


Fig. 4 Density-temperature isobars of the present three-species kerosene surrogate.

represented by those of single reference fluids. Because only few simple fluids follow this corresponding states principle very accurately, the extended corresponding states principle adds one more parameter called “acentric factor” to account for the deviation of molecular shape from sphere and the effect of molecular dipole moment. The Benedict–Webb–Rubin equation of states was used to evaluate the properties of the reference fluid.<sup>38</sup>

Figure 4 shows the calculated density-temperature isobars of the present kerosene surrogate at different pressures. The measured kerosene densities at relatively low temperature range, which were reported previously,<sup>39</sup> are also plotted in Fig. 4 for comparison. It is seen that the computed results agree well with the experimental data available. The calculated bubble point and dew point for the surrogate are respectively 423 and 437 K, which are comparable to the measured values of 415 and 452 K. In addition, the calculated critical pressure and critical temperature are 24 atm and 613 K, while the critical conditions of common kerosene are approximately 22 atm and 630 K. The data shown in Fig. 4 for temperature higher than the thermal cracking limit of  $\sim 750$  K are included only for illustration purposes.

Calculations also showed that near the critical point the speed of sound, viscosity, and thermal conductivity of the kerosene surrogate decrease to those corresponding to the gas phase, while its heat capacity and specific heats increase dramatically. Considering the temperature and pressure in the fuel delivery system of practical scramjet engines could be supercritical or near the critical point, the accurate determination of the fuel properties is imperative for optimal design and effective control of the fuel system.

## Results and Discussion

### Flow-Rate Calibration

For the experiments using liquid atomization, the mass flow rate of liquid kerosene was determined with an orifice plate flowmeter. Calibration was carried out by measuring the actual amount of kerosene discharge within a given time duration. Figure 5 shows that at room temperature the mass flow rate of liquid kerosene varies linearly with the square root of the differential pressure across the orifice.

For the flow-rate measurement of kerosene vapor, the use of an orifice flowmeter becomes somewhat complicated because the thermophysical properties of heated kerosene change rapidly with pressure and temperature, especially when approaching the critical point. However, similar to a gas, a fluid at supercritical state can be accelerated to sonic speed as long as there is no condensation during acceleration. Therefore, the flow rates of a supercritical fluid can be measured with a sonic nozzle. The use of sonic nozzle eliminates the influence of backpressure when the sonic condition is maintained at the nozzle throat. Such a choking condition also facilitates the calculations of kerosene vapor flow rates using SUPERTRAPP. Applying the assumption of isentropic acceleration, the properties of kerosene surrogate at sonic condition corresponding to the fuel stagnation condition can be calculated. For the present kerosene sur-

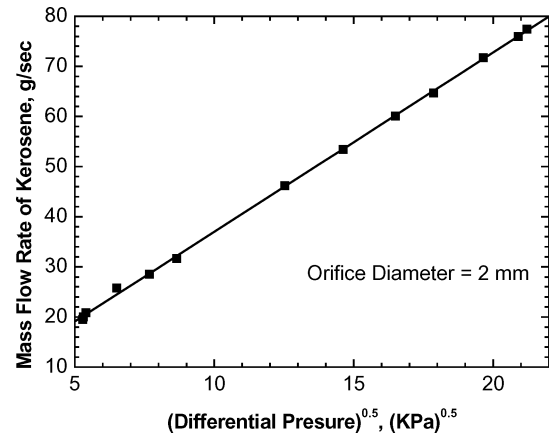


Fig. 5 Calibration of liquid kerosene mass flow rate with an orifice plate flowmeter.

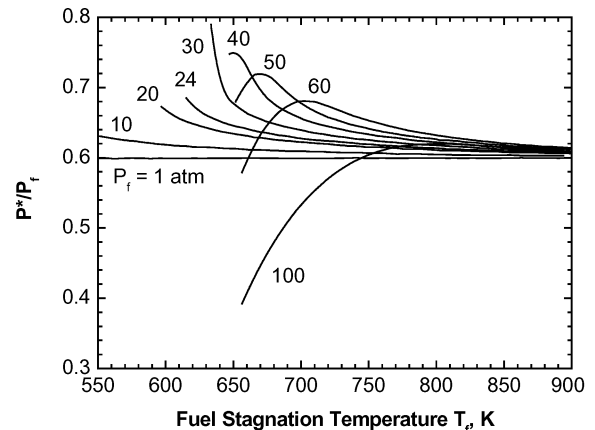


Fig. 6 Computed ratio of pressure at sonic condition  $P^*$  and fuel stagnation pressure  $P_f$  as functions of fuel stagnation temperature  $T_f$  and  $P_f$  using the present three-species kerosene surrogate.

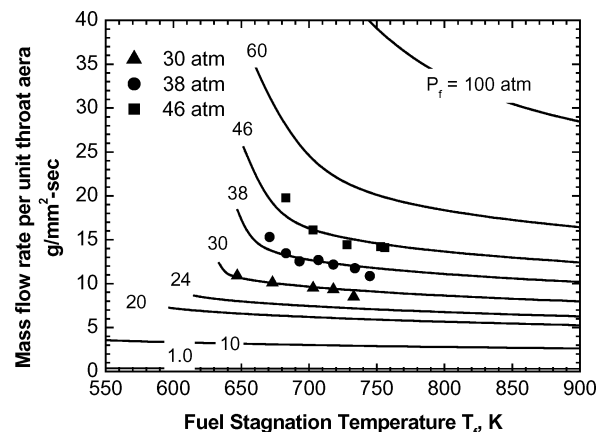


Fig. 7 Comparison of experimental (China no. 3 aviation kerosene) and computational (the present three-species kerosene surrogate) mass flow rates per unit throat area at various fuel stagnation conditions.

rogate, Fig. 6 shows the computed ratio of the fluid pressure at the choked throat (Mach one)  $P^*$  to the fuel stagnation pressures  $P_f$  as a function of fuel stagnation temperature  $T_f$  at varying fuel stagnation pressures. The computed results clearly demonstrate that the  $P^*/P_f$  ratio is very sensitive to  $T_f$  variations when the injection pressure is close to and greater than the critical pressure (24 atm). Figure 7 further plots the computed mass flow rate of kerosene surrogate per unit throat area as functions of  $P_f$  and  $T_f$ .

The procedure to determine the actual amount of kerosene vapor discharge is similar to that employed for liquid-kerosene injection.

A vapor-collecting system is instrumental in the success of accurate calibration, which was accomplished by using the condenser of an air conditioner. The measured flow rates per unit throat area at fuel injection pressures of 30, 38, and 46 atm, denoted as symbols, are included in Fig. 7 for comparison. It is seen from Fig. 7 that the theoretical calculations using the surrogate fuel are in good agreement with the measured values using China no. 3 aviation kerosene for fuel temperature below 750 K. When the fuel temperature exceeds 750 K, the computed mass flow rates can no longer be used because thermal cracking will lead to the changes in mixture composition as well as the corresponding thermophysical properties. Overall, the uncertainty associated with the determination of kerosene mass flow rate is approximately 5% by taking the measurement accuracies of the throat area, injection pressure, and fuel temperature into account.

### Phase Diagram of Kerosene Surrogate

The thermodynamic modeling of the kerosene surrogate can also shed light on the understanding of physical processes associated with different injection modes. Figure 8 is the phase diagram obtained using the present three-species surrogate. The transitions of fuel states related to pure liquid-kerosene injection and supercritical kerosene injection are illustrated and compared in the following.

Assuming a Mach 7–8 flight condition, the static temperature at the inlet of a practical scramjet combustor is estimated to be

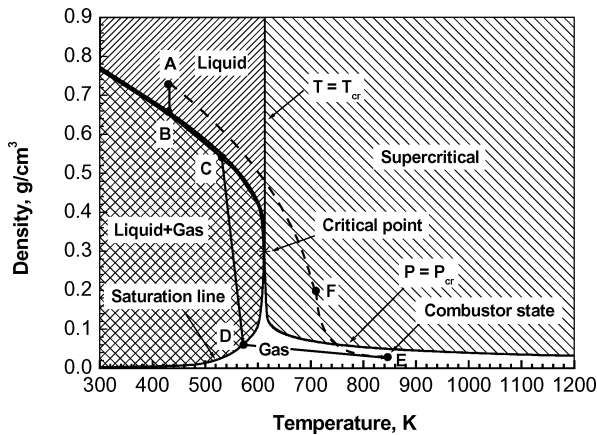


**Fig. 8** Phase diagram for the present kerosene surrogate demonstrating the processes with liquid fuel injection (A → B → C → D → E) and supercritical fuel injection (A → F → E).

around 830 K, while the combustor inlet pressure is typically subatmospheric.<sup>2</sup> This combustor state is then denoted as point E in Fig. 8. Depending on the pressure and temperature of kerosene, the injected fuel would experience changes in different thermodynamic states from the injection condition to the combustor condition.

Considering the injection of liquid kerosene with a supercritical pressure (point A in Fig. 8) into the combustor with state E, the fuel would first undergo a sudden decrease in pressure (A → B), where atomization process commences. As the fuel droplet temperature is heated up to be above the bubble point (B → C), fuel vaporization occurs (C → D). The temperature of fuel vapor will continue to increase until reaching the static temperature in the combustor following D → E in Fig. 8.

For the case of supercritical kerosene injection, the transition of A → F shown in Fig. 8 corresponds to the scenario that the liquid fuel is first heated to supercritical temperature under supercritical pressure, while the transition of F → E relates to the injection process. For such a supercritical fuel injection, because the fuel latent heat is zero, it can transform continuously into the gas phase without an interface. This direct fuel transformation into gas phase without involving atomization and vaporization processes is expected to enhance fuel-air mixing and subsequently facilitate self-ignition of kerosene.

Furthermore, Fig. 8 along with Fig. 4 suggests that it is advantageous to apply supercritical pressure for heated kerosene injection. When the injection pressure is subcritical, two-phase flow will be present in the kerosene heating/delivery system. The resulting two-phase flow would complicate the fuel flow rate measurements and lead to difficulties in flow control. Hence, supercritical injection pressure was employed for all of the experiments carried out in this investigation.

Using the present kerosene delivery/heating/injection system, a series of experiments were conducted to characterize the injection processes, fuel-air mixing, and combustor performance, under a wide range of injection conditions, which will be presented in the following text.

### Characterization of Heated Kerosene Jets into Quiescent Atmosphere

To provide insight into the injection conditions for the supersonic combustor investigation, a set of experiments was carried out to characterize the kerosene jet structure at varying preheat temperatures with a fixed supercritical injection pressure. With a given injection pressure of 4 MPa, Fig. 9 compares the direct images of four kerosene jets into quiescent atmosphere at fuel temperatures of 290, 480, 510, and 550 K, respectively. The orifice diameter of

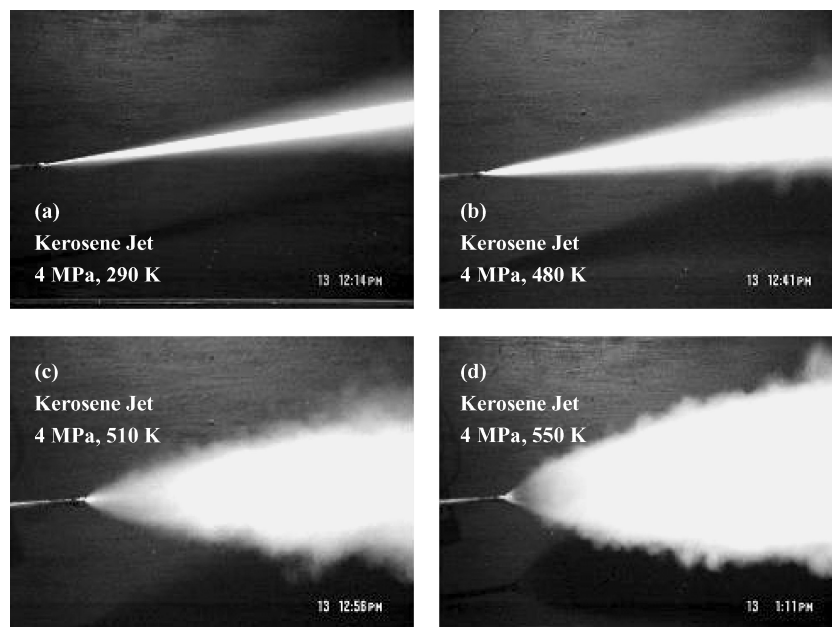


**Fig. 9** Direct images of pressurized kerosene jet into quiescent atmosphere at different injection temperatures.

fuel injector was 0.8 mm. It is seen that the heated kerosene jet first exhibited mixed liquid/vapor plume at injection temperature of 480 K, as shown in Fig. 9b. However, at this condition the amount of kerosene vapor was much less than that of liquid phase. Further increasing the fuel temperature to 510 K, Fig. 9c illustrates that vaporized kerosene dominated the jet structure, while little amount of liquid kerosene spray was still noted. Figure 9d clearly shows that the heated kerosene nearly completely turned into vapor phase at 550 K preheat temperature. Especially, “white smoke” was observed even right at the injector exit. We note that the fuel was injected at a supercritical pressure, while the ambient pressure and temperature in Fig. 9 were much lower than the critical values. As a result, the fuel vapor condensed into liquid droplets as its temperature decreased. The increase in plume angle with increasing injection temperature demonstrated in Fig. 9 is a result of enhanced vaporization, which would in turn promote the overall fuel-air mixing.

#### Characterization of Heated Kerosene Jets into a Supersonic Crossflow

For visualization experiments of nonreacting kerosene jet structures in a supersonic crossflow, the cavity flame-holder was replaced by a flat-plate module with only one injection orifice of 0.8 mm. Four kerosene jets with the same injection conditions as those of Fig. 9 were visualized by injecting into a Mach 2.5 crossflow. The local static temperature and pressure at the test section are 570 K and 0.07 MPa, respectively. Figure 10 shows the corresponding schlieren images. It is seen that the heated kerosene jet structure was severely bent by the Mach 2.5 crossflow, and the bow shock ahead of the jet was evident. The penetration depths of four kerosene jets were approximately the same in the fuel temperature range of 290–550 K. This further implies that the resulting jet momentums were quite similar as a consequence of the same applied injection pressure.

For the case of pure liquid atomization shown in Fig. 10a, the spray structure in the schlieren image appeared to be dark owing to the blockage of incident light by the fine droplets. As the temperature of kerosene was increased to 480 K, the blockage of incident light by the kerosene spray, while still noticeable, was substantially reduced, as seen in Fig. 10b. Further increasing kerosene temperature beyond 500 K, Figs. 10c and 10d clearly show that the heated kerosene jet structures became more and more transparent to the incident light. Obviously, this “transparency” is an indicative of the greater extent of kerosene gasification. The fuel-air mixing time is also expected to be reduced as a consequence of this enhanced atomization/vaporization with increased fuel temperature. The present results demonstrate that it is feasible to achieve complete vaporization of kerosene and to inject vaporized kerosene into a supersonic com-

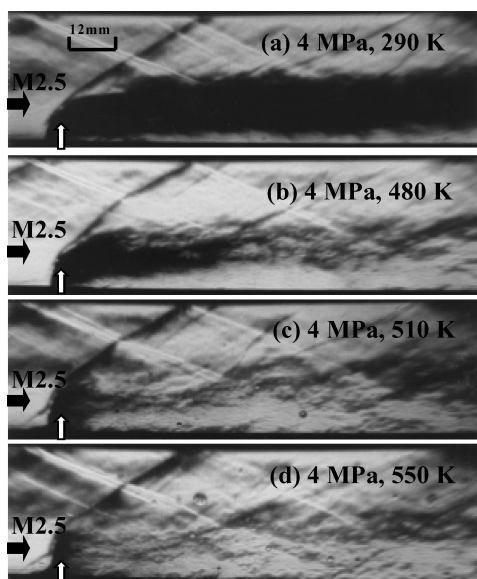


Fig. 10 Schlieren images of pressurized kerosene jet into a Mach 2.5 crossflow at different injection temperatures. The local static temperature and pressure were respectively 570 K and 0.07 MPa.

bustor with comparable penetration depth as the liquid jet. Because the use of vaporized kerosene injection bypasses the vaporization process completely, the performance of a supersonic combustor is expected to be improved significantly, which will be demonstrated in due course.

#### Effects of Supercritical Fuel Injection on Combustor Performance

To assess the effects of supercritical kerosene injection on combustor performance, a series of experiments were conducted in a Mach 2.5 model combustor. The results were also compared to those obtained using pure liquid injection and effervescent atomization. All experiments were conducted under approximately identical flow conditions, that is, a stagnation temperature of  $\sim 1750$  K and a stagnation pressure of  $\sim 1.15$  MPa. The static temperature and static pressure in the combustor were respectively  $\sim 800$  K and  $\sim 0.07$  MPa, which would simulate a Mach 6 scramjet engine conditions. Although aviation kerosene was used in experiments, the mass flow rate of supercritical kerosene at the given injection condition was determined based on the calculations of surrogate fuel shown in Fig. 7.

To facilitate self-ignition of kerosene in the supersonic combustor, a small amount of pilot hydrogen was used. Following the definition of Ref. 26, the equivalence ratio of pilot hydrogen  $\phi_H$  and the effective equivalence ratio of kerosene  $\phi_f$  are determined based on the assumption that hydrogen is first consumed completely with the available oxygen and kerosene is then oxidized by the remaining air. In both liquid and vaporized injection cases the amount of pilot hydrogen ranges from 0.07–0.1.

Figure 11 compares the typical static-pressure distributions along the axial direction in the model combustor using supercritical kerosene injection and liquid-kerosene atomization. The relative locations of kerosene injection, pilot hydrogen injection, and cavity flame-holder are also sketched in Fig. 11. For combustion of liquid kerosene, the fuel was injected at room temperature and under pressure of 1.9 MPa. For combustion of supercritical kerosene, the fuel prior to injection was preheated to a desired temperature, ranging from 730 to 740 K, under a supercritical pressure of 3.8 MPa. In both injection schemes, kerosene was injected at the similar global equivalent ratio  $\phi_f$  of 0.37–0.38. Figure 11 clearly shows a significant increase in overall pressure level during combustion when using supercritical fuel injection. Although pilot hydrogen also contributes to the static-pressure rise, the amount of pilot hydrogen employed for the case of supercritical kerosene injection is less. In addition, Fig. 11 demonstrates that the experimental data of supercritical kerosene injections were highly repeatable within the experimental uncertainty.

A one-dimensional model, which was developed in Ref. 40, was applied to assess the combustor performance. In this model, the flow-field within the combustor is approximated based on the measured static-pressure distribution.<sup>40</sup> Although the complex interactions of

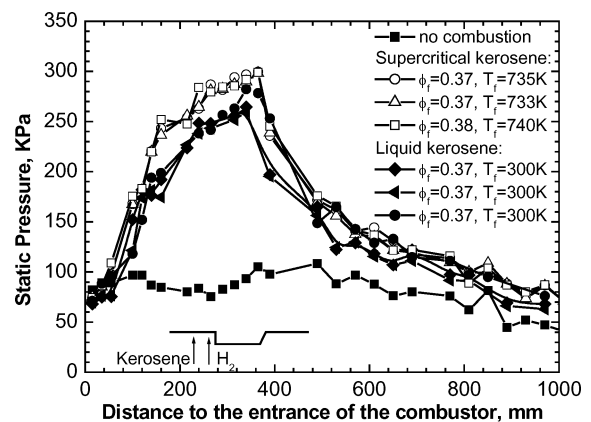
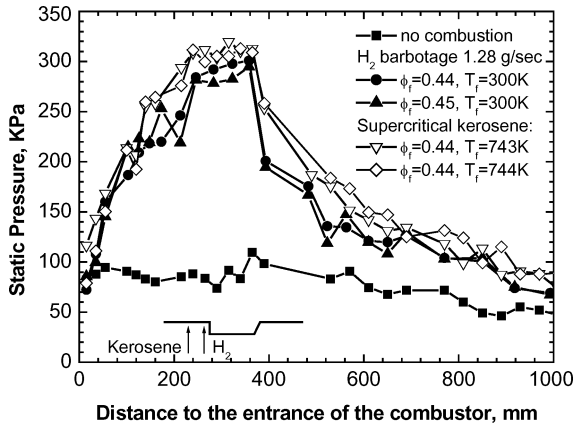


Fig. 11 Comparison of static-pressure distributions with supercritical and liquid-kerosene injections. Vitiated Mach 2.5 air: stagnation temperature was around 1750 K, and stagnation pressure was about 1.15 MPa.



**Fig. 12** Comparison of static-pressure distributions for the cases using supercritical kerosene injection and effervescent atomization with hydrogen barbotage. Vitiated Mach 2.5 air; stagnation temperature was around 1750 K, and stagnation pressure was about 1.15 MPa.

shocks, expansion waves, and boundary layers are not accounted for in this simplified model, the approximate flowfield is seen to be consistent with the experimental observation. Furthermore, this one-dimensional model greatly facilitates data analyses. The effect of pilot hydrogen is included in the analysis when calculating the adiabatic flame temperature. Applying the one-dimensional model, it was found that the overall combustion efficiencies for the liquid-kerosene cases were approximately 65–75%, whereas those for the supercritical kerosene cases were improved to approximately 86–88%. Therefore, the use of supercritical kerosene injection is shown to increase the combustion efficiency substantially.

Combustor performance of supercritical kerosene was further compared to that of effervescent atomization with hydrogen barbotage.<sup>27,28</sup> Figure 12 compares the measured static-pressure profiles with a given overall kerosene equivalence ratio. The supercritical kerosene was injected at temperature of about 740 K and pressure of 4.6 MPa, while the liquid kerosene was injected at room temperature and under pressures of 2.5–3.5 MPa with barbotaged hydrogen of 1.28 g/s. The global kerosene equivalent ratios  $\phi_f$  in these experiments were 0.44–0.45. It is seen from Fig. 12 that the static pressures of supercritical kerosene combustion were slightly higher. On the average, the combustion efficiency of supercritical kerosene was approximately 87%, which was slightly higher than the averaged combustion efficiency of 84% for liquid fuel with hydrogen barbotage.

## Conclusions

Characteristics of kerosene combustion in a Mach 2.5 model combustor using vaporized kerosene injection at various preheat temperatures, and injection pressures were experimentally investigated. A two-stage heating system with minimum fuel coking was designed and tested. The kerosene delivery system developed was able to support different injection modes, from liquid fuel injection to supercritical fuel injection.

A three-species surrogate was selected to simulate the thermo-physical properties of the China no. 3 aviation kerosene over a wide range of pressures and temperatures relevant to the experimental conditions. The calculated densities and mass flow rates per unit throat area of the present surrogate were shown to agree well with the limited experimental data available. Hence, the calculated results were used to guide the selection of experimental conditions and the control of kerosene flow rates.

Schlieren results characterizing different kerosene jets into a Mach 2.5 crossflow demonstrated that the fuel state was essentially in vapor phase at an injection pressure of 4 MPa and preheat temperatures beyond 550 K, while the penetration depth remained essentially unchanged as compared to the liquid-kerosene atomization case applying the same injection pressure. Combustion tests showed that the static-pressure profiles for combustion of supercritical kerosene were significantly higher than those of liquid

kerosene and also slightly higher than those using effervescent atomization with hydrogen barbotage. Correspondingly, the combustion efficiency of supercritical kerosene can be 10–15% higher than that of liquid kerosene, whereas it is considered to be comparable to that using effervescent atomization with hydrogen barbotage.

Because the increase in adiabatic flame temperature caused by fuel preheating is not substantial, the improvement in combustor performance by using supercritical kerosene injection is mainly caused by the elimination of the atomization and vaporization processes and increase in fuel-air mixing level. Recognizing that the combustor performance can be also affected by different factors, such as Mach number, cavity flame-holder geometry, fuel injection scheme, and combustor configuration, further parametric investigation on the use of supercritical kerosene is warranted.

## Acknowledgments

The current research program of the Chinese Academy of Sciences was supported by the National Natural Science Foundation of China under Contract 10232060. The authors would like to acknowledge X. N. Lu for the assistance in designing and testing the kerosene heater. We also thank D. X. Qian and Y. Li for the technical support.

## References

- Edwards, T., "Liquid Fuel and Propellant for Aerospace Propulsion: 1903-2003," *Journal of Propulsion and Power*, Vol. 19, No. 6, 2003, pp. 1089–1107.
- Tishkoff, J. M., Drummond, J. P., Edwards, T., and Nejad, A. S., "Future Direction of Supersonic Combustion Research: Air Force/NASA Workshop on Supersonic Combustion," AIAA Paper 97-1017, Jan. 1997.
- Maurice, L., and Edwards, T., "Liquid Hydrocarbon Fuels for Hypersonic Propulsion," *Scramjet Propulsion*, edited by E. T. Curran, and S. N. B. Murthy, Progress in Astronautics and Aeronautics, Vol. 189, AIAA, Reston, VA, 2001, pp. 757–822.
- Vinogradov, V., Kobigsky, S., and Petrov, M., "Experimental Investigation of Liquid Carbonhydrogen Fuel Combustion in Channel at Supersonic Velocities," AIAA Paper 92-3429, July 1992.
- Bonghi, L., Dunlap, M. J., Owens, M. G., Young, C., and Segal, C., "Hydrocarbon Piloted Energy for Supersonic Combustion of Liquid Fuels," AIAA Paper 95-0730, Jan. 1995.
- Segal, C., Owens, M. G., Tehrani, S., and Vinogradov, V., "Flame-Holding Configurations for Kerosene Combustion in a Mach 1.8 Airflow," AIAA Paper 97-2888, July 1997.
- Baurle, R. A., and Gruber, M. R., "A Study of Recessed Cavity Flow-Fields for Supersonic Combustion Applications," AIAA Paper 98-0938, Jan. 1998.
- Gruber, M. R., Baurle, R. A., Mathur, T., and Hsu, K.-Y., "Fundamental Studies of Cavity-Based Flameholder Concepts for Supersonic Combustors," *Journal of Propulsion and Power*, Vol. 17, No. 1, 2001, pp. 146–153.
- Ben-Yakar, A., and Hanson, R. K., "Cavity Flame-Holders for Ignition and Flame Stabilization in Scramjets: An Overview," *Journal of Propulsion and Power*, Vol. 17, No. 4, 2001, pp. 869–877.
- Yu, K., Wilson, K. J., and Schadow, K. C., "Effect of Flame-Holding Cavities on Supersonic-Combustion Performance," *Journal of Propulsion and Power*, Vol. 17, No. 6, 2001, pp. 1287–1295.
- Mathur, T., and Billig, F., "Supersonic Combustion Experiments with a Cavity-Based Fuel Injector," *Journal of Propulsion and Power*, Vol. 17, No. 6, 2001, pp. 1305–1312.
- Arai, T., and Schetz, J. A., "Injection of Bubbling Liquid Jet from Multiple Injectors into Supersonic Stream," *Journal of Propulsion and Power*, Vol. 10, No. 3, 1994, pp. 382–386.
- Lin, K.-C., Kirkendall, K. A., Kennedy, P. J., and Jackson, T. A., "Spray Structures of Aerated Liquid Fuel Jets in Supersonic Crossflows," AIAA Paper 99-2374, July 1999.
- Avrashkov, V., Baranovsky, S., and Levin, V., "Gasdynamic Feature of Supersonic Kerosene Combustion in a Model Combustor Chamber," AIAA Paper 99-5268, Oct. 1999.
- Mathur, T., Lin, K.-C., Kennedy, P. J., Gruber, M., Donbar, J., Jackson, T., and Billig, F., "Liquid JP-7 Combustion in a Scramjet Combustor," AIAA Paper 2000-3581, July 2000.
- Yanovskii, L. S., Sapgir, G. B., Strokin, V. N., and Ivanov, V. F., "Endothermic Fuels: Some Aspects of Fuel Decomposition and Combustion at air Flows," International Symposium on Air Breathing Engines, Paper 99-7067, Sept. 1999.
- Bruno, C., Filippi, M., and Czysz, P. A., "Hydrocarbon Fuels Reforming for Hypersonic Propulsion," International Symposium on Air Breathing Engines, Paper 99-7237, Sept. 1999.

- <sup>18</sup>Colket, M. B., and Spadaccini, L. J., "Scramjet Fuels Autoignition Study," *Journal of Propulsion and Power*, Vol. 17, No. 2, 2001, pp. 315–323.
- <sup>19</sup>Kay, I. W., Peshke, W. T., and Guile, R. N., "Hydrocarbon-Fueled Scramjet Combustor Investigation," *Journal of Propulsion and Power*, Vol. 8, No. 2, 1992, pp. 507–512.
- <sup>20</sup>Jackson, K., Corporan, E., Buckley, P., Leingang, J., Karpuk, M., Dippo, J., Hitch, B., Wickham, D., and Yee, T., "Test Results of an Endothermic Fuel Reactor," AIAA Paper 95-6028, April 1995.
- <sup>21</sup>Morris, C. Q., Campbell, R. L., Edelman, R. B., and Jaul, W. K., "Hydrocarbon Fueled Dual-Mode Ramjet/Scramjet Concept Evaluation," *Proceedings of the International Symposium on Air Breathing Engines*, ISABE Paper 97-7053, Sept. 1997.
- <sup>22</sup>Owens, M., Segal, C., and Auslender, A. H., "Effects of Mixing Schemes on Kerosene Combustion in a Supersonic Airstream," *Journal of Propulsion and Power*, Vol. 13, No. 4, 1997, pp. 525–531.
- <sup>23</sup>Kimura, I., Aoki, H., and Kato, M., "The Use of a Plasma Jet for Flame Stabilization and Promotion of Combustion in Supersonic Air Flows," *Combustion and Flame*, Vol. 42, 1981, pp. 297–305.
- <sup>24</sup>Kitagawa, T., Moriwaki, A., Murakami, K., Takita, K., and Masuya, G., "Ignition Characteristics of Methane and Hydrogen Using a Plasma Torch in Supersonic Flow," *Journal of Propulsion and Power*, Vol. 19, No. 5, 2003, pp. 853–858.
- <sup>25</sup>Cross, M. A., Sanders, D. D., O'Brien, W. F., and Schetz, J. A., "Operation of a Plasma Torch for Supersonic Combustion Applications with a Simulated Cracked JP-7 Feedstock," AIAA Paper 2003-6935, Dec. 2003.
- <sup>26</sup>Yu, G., Li, J. G., Zhang, X. Y., Chen, L. H., and Sung, C. J., "Investigation of Kerosene Combustion Characteristics with Pilot Hydrogen in Model Supersonic Combustors," *Journal of Propulsion and Power*, Vol. 17, No. 6, 2001, pp. 1263–1272.
- <sup>27</sup>Yu, G., Li, J. G., Chang, X. Y., Chen, L. H., and Sung, C. J., "Fuel Injection and Flame Stabilization in a Liquid-Kerosene-Fueled Supersonic Combustor," *Journal of Propulsion and Power*, Vol. 19, No. 5, 2003, pp. 885–893.
- <sup>28</sup>Yu, G., Li, J. G., Zhao, J. R., Yue, L. J., Chang, X. Y., and Sung, C. J., "An Experimental Study of Kerosene Combustion in a Supersonic Model Combustor Using Effervescent Atomization," *Proceedings of the Combustion Institute*, Vol. 30, 2005, pp. 2859–2866.
- <sup>29</sup>Yang, V., "Modeling of Supercritical Vaporization, Mixing and Combustion Processes in Liquid-Fueled Propulsion System," *Proceeding of the Combustion Institute*, Vol. 28, 2000, pp. 925–942.
- <sup>30</sup>Edwards, T., and Maurice, L. Q., "Surrogate Mixtures to Represent Complex Aviation and Rocket Fuels," *Journal of Propulsion and Power*, Vol. 17, No. 2, 2001, pp. 461–466.
- <sup>31</sup>Dagaut, P., "On the Kinetics of Hydrocarbon Oxidation from Natural Gas to Kerosene and Diesel Fuel," *Physical Chemistry Chemical Physics*, Vol. 4, No. 11, 2002, pp. 2079–2094.
- <sup>32</sup>Violi, A., Yan, S., Eddings, E. G., Sarofim, A. F., Granata, A., Faravelli, T., and Ranzi, E., "Experimental Formulation and Kinetic Model for JP-8 Surrogate Mixtures," *Combustion Science and Technology*, Vol. 174, Sept.–Dec. 2002, pp. 399–417.
- <sup>33</sup>Montgomery, C. J., Zhao, W., Tam, C. J., Eklund, D. R., and Chen, J. Y., "CFD Simulations of a 3-D Scramjet Flameholder Using Reduced Chemical Kinetic Mechanisms," AIAA Paper 2004-3874, July 2004.
- <sup>34</sup>Mawid, M. A., Park, T. W., Sekar, B., and Arana, C., "Importance of Surrogate JP-8/Jet-A Fuel Composition in Detailed Chemical Kinetics Development," AIAA Paper 2004-4207, July 2004.
- <sup>35</sup>Li, J. G., Yu, G., Zhang, Y., Li, Y., and Qian, D. X., "Experimental Studies on Self-Ignition of Hydrogen/Air Supersonic Combustion," *Journal of Propulsion and Power*, Vol. 13, No. 4, 1997, pp. 538–542.
- <sup>36</sup>Ely, J. F., and Huber, M. L., "NIST Standard Reference Database 4—NIST Thermophysical Properties of Hydrocarbon Mixtures," National Inst. of Standards, Gaithersburg, MD, Feb. 1990.
- <sup>37</sup>Fisher, G. D., and Leland, T. W., "The Corresponding States Principle Using Shape Factors," *Industrial and Engineering Chemistry Fundamentals*, Vol. 9, No. 4, 1970, pp. 537–544.
- <sup>38</sup>Jacobsen, R. T., and Stewart, R. B., "Thermodynamic Properties of Nitrogen Including Liquid and Vapor Phases from 63 K to 2000 K with Pressures to 10,000 bar," *Journal of Physical and Chemical Reference Data*, Vol. 2, No. 4, 1973, pp. 757–922.
- <sup>39</sup>Yu, G., Li, J. G., Zhao, Z., Chang, X. Y., and Sung, C. J., "Investigation of Vaporized Kerosene Injection in a Supersonic Model Combustor," AIAA Paper 2003-6938, Dec. 2003.
- <sup>40</sup>Yu, G., Li, J. G., Zhang, X. Y., Chen, L. H., Han, B., and Sung, C. J., "Experimental Investigation on Flameholding Mechanism and Combustion Performance in Hydrogen-Fueled Supersonic Combustors," *Combustion Science and Technology*, Vol. 174, No. 3, 2002, pp. 1–27.